Thermomechanical properties and deformation behavior of a unidirectional carbon-fiber-reinforced shape memory polymer composite laminate

Xin Lan [ORCID],[1] Liwu Liu,[2] Yanju Liu,[2] Jinsong Leng[1]

[1]Center for Composite Materials, Harbin Institute of Technology (HIT), Harbin 150080, People's Republic of China
[2]Department of Aerospace Science and Mechanics, Harbin Institute of Technology (HIT), Harbin 150001, People's Republic of China
Correspondence to: X. Lan (E-mail: lanxin@hit.edu.cn), and J. Leng (E-mail: lengjs@hit.edu.cn)

ABSTRACT: A shape memory polymer (SMP) demonstrates large reversible deformation functionality upon exposure to heating stimuli. In this study, the thermomechanical properties and deformation behavior of a unidirectional carbon-fiber-reinforced SMP composite (SMPC) laminate were studied. The findings can be used as a basis to design angle-ply laminated plates, woven laminated plates, or special laminated structures used for space deployment. The fundamental static and dynamic mechanical properties of SMP and SMPC were characterized. The fiber-reinforced SMPC exhibited local postmicrobuckling behavior and obtained a high-reversible macroscale strain of 9.6%, which enabled the high-reversible deformation to be used for foldable structures in space. The state of critical failure of bending deformation was determined through microscale morphology observations and provided the upper limit in the design of SMPC structures. The evolution of the key shape memory properties (e.g., recovery speed and recovery ratio) during deformation cycles was characterized, and it offered the general recovery performance of a space deployable structure. © 2019 Wiley Periodicals, Inc. J. Appl. Polym. Sci. **2019**, *136*, 48532.

INTRODUCTION

The use of shape memory polymers (SMPs) as multifunctional materials has elicited much research attention.[1–3] SMPs have dual shape features, namely, original and deformed shapes. Compared with traditional polymers, SMPs possess a unique reversible phase that freezes the deformed shape below the transition temperature (T_s) and releases it toward the original shape at a temperature above T_s.[2] Hence, SMPs exhibit stimulus-responsive[4] and large reversible deformation[5] functionality upon exposure to external Joule heating stimuli (e.g., electricity, magnetism, and light) through the incorporation of functional fillers (e.g., carbon black,[6] carbon nanotubes,[5,7,8] carbon nanofibers,[9] graphene,[10] and nickel powder[11,12]). The associated potential applications include 4D printing,[13–15] biomedicine,[16] foldable origami structures,[17,18] soft electronics,[19,20] and self-healing or self-repairing microsystems.[21]

By designing the secondary crosslinked network architectures (mechanism, comonomers, and initiator, etc.) on side chains or chain segments linking two chemical netpoints, the temporary

stabilization (predeformed shape) of thermosetting SMP could form through the aggregation of switching polymer segments.[1,2,22,23] When reheating, by detaching the secondary crosslinked segments, the stored strain energy is released, and the macroscale shape recovery of thermosetting SMP is realized (recovered shape). The thermomechanical properties of three SMPs, namely, styrene-based, epoxy-based, and cynate-based SMPs, as thermosetting SMPs have been determined and compared.[24,25] The general values of glass transition temperature (T_g), elastic modulus at room temperature, and elongation limits at T_g were established, respectively, as follows: 40–90 °C, 1–3 GPa, and 100–120% for styrene-based SMP; 100–170 °C, 3–4 GPa, and 40–60% for epoxy-based SMP; and 180–250 °C, 2.5–3.5 GPa, and 20–40% for cynate-based SMP.[2,25] Compared with styrene-based SMP, epoxy-based SMP has a higher T_g, higher elastic modulus, and lower but acceptable deformation limits (i.e., 20–40%) for morphing structures. However, the overall mechanical properties are unsatisfactory; thus, epoxy-based SMPs cannot be used as structural materials, such as aerospace morphing[25] and space deployable structures.[26] These materials need to be mechanically reinforced as shape memory polymer composites (SMPCs) by

incorporating fibers.[25,26] Reinforced fibers usually include carbon, glass, and other types of fibers, such as cover chopped, unidirectional, and woven fabric.[2] SMPC filled with chopped fibers achieves a relatively limited improvement in mechanics and still exhibits large reversible deformation. An SMP (e.g., poly(styrene-b-butadiene-b-styrene) triblock and linear low-density polyethylene filled with chopped glass fibers has a high elasticity modulus (50 MPa for pure SMP and 110 MPa for SMPC with 2.5 wt % chopped fibers), and the associated strain limit decreases from 5.5 to 3%.[27] Similar trends and results have been reported for other types of SMPs reinforced by chopped glass[28,29] and carbon[30] fibers. In summary, for short fiber-filled SMPs, the balance between fiber content and the overall mechanical and shape memory performance (including elasticity modulus, strength, reversible deformation limit, and shape recovery ratio) under numerous deformation cycles should be considered.[26,29] Short fiber-filled SMPs are commonly used as functional materials (e.g., sensing).

Continuous fiber-reinforced SMPC demonstrates good mechanical performance and possesses high recovery stress but low reversible strain; it contains unidirectional fiber, angle-ply, and woven laminates.[30–32] For the unidirectional fiber-reinforced SMPC laminate, the mechanical and shape memory properties are the basic parameters for designing angle-ply laminated plates, woven laminated plates, and other special laminated SMPC structures with large deformation capacity. However, studies related to this topic are scarce because conventional preparation procedures (e.g., compression molding, resin-transfer molding, tape laying, and filament winding) are difficult to realize when new materials of SMP resin developed in recent years are used.[33] When woven fibers are utilized, SMPC can be prepared through manual cloth laying, which does not require SMP processing parameters, such as dynamic viscosity and flowability. For woven fabric-reinforced SMPC, epoxy-based SMP with 38 vol % woven glass fiber fabric demonstrates enhanced stress recovery by two orders of magnitude compared with pure epoxy-based SMP under flexural deformation.[32] The effect of asymmetric layering in the thickness direction of SMPC produces different shape memory effects. During flexural deformation, SMPC with abundant carbon fiber at the outer side in the tensional state achieves a higher shape recovery ratio and stress than SMPC with abundant carbon fiber at the inner side in the compressive state under the same filler content.[33]

The influence of fatigue and failure on the shape memory effect has also been investigated. Delamination and debonding among fabric layers and fiber breaking are the main factors in the reduction of maximum reversible strain, shape recovery ratio, and force.[34]

On the basis of fiber-reinforced SMPC materials, deformable composite structures containing SMPs have also been proposed to explore special properties (e.g., variable stiffness) and associated applications (e.g., aircraft morphing structures).[25,35] Hybrid layered beams consisting of woven carbon fiber-reinforced polymer composites and SMP layers have been tailored to explore the bending deformation capacity and failure behavior. By controlling the temperature, the flexural stiffness of these layer SMPC beams can be effectively designed for direct use as aircraft morphing structures.[36,37] To increase the flexural deformation limit of SMPC sandwich panels made from thermosetting epoxy-based SMP and its foam, a previous study[38] used non-shape-memory resin with relatively high stiffness on the inner compression surface to prevent the neutral surface from moving toward the outer tensional surface at an elevated temperature upon bending; in this manner, the buckling fibers within the SMP resin with relatively low stiffness on the inner side would not suffer from a large strain, which causes the failure of SMPC composites. Without SMPs, the shape memory effect can be alternatively realized by interleaved composite structures composed of conventional epoxy-based/carbon-fiber laminates and polystyrene interleaf layers.[39] Several novel space deployable structures[40] and release devices have been developed by using fabric-/carbon fiber-reinforced SMPCs and their special structures.[31] However, the thermomechanical properties and deformation behavior of unidirectional fiber-reinforced SMPC laminates have received minimal attention as a basis for the design of space-deployable SMPC angle-ply laminated plates, woven laminated plates, and special laminated structures.[32–34,41–43]

In this study, a unidirectional carbon fiber-reinforced SMPC laminate was fabricated by using epoxy-based SMP synthesized by the authors' group.[44] To use SMPC in actual space-deployable structures, this study characterized the basic mechanical and shape memory properties of epoxy-based SMP and its composite material laminate according to related aerospace standards. The basic mechanical and shape memory properties included static and dynamic mechanical properties, bending deformation behavior of SMPC due to microbuckling, and shape memory performance. On the basis of this fundamental study on unidirectional fiber-reinforced epoxy-based SMPC, angle-ply laminated plates, woven laminated plates, and several special laminated structures can be designed for use in next-generation deployable structures in space, such as deployable soft solar arrays and solar wind and lens hoods.

SMP PREPARATION AND EXPERIMENTAL METHODS

SMP and SMPC Preparation

SMP and carbon fibers. Epoxy-based SMPs were previously synthesized by the author's research group.[44] In this study, one type of composition was selected as the SMP matrix for the SMPC composite. With the aim of satisfying the demand in space environments, this epoxy-based SMP was specially modified, thus laying a foundation for use as a deployable structure in space. This SMP was synthesized as follows: an epoxy-based resin, a curing agent, and an accelerant were mixed at a mass ratio of 100:80:3.6. To improve the ability to resist the space environment, an active linear epoxy monomer with long C—O bond chains was added to the resin. The active linear monomer and epoxy-based resin have the following optimized chemical dose rate: group number ratio of 1:1 and molecular weight ratio of 2:5. This unique linear epoxy monomer, also acting as a molecular switch in the thermoset crosslinked network, endows the shape memory effect to the epoxy-based SMP, which is different from traditional thermoset epoxy resin without a shape memory effect. The solidification process proceeded through the following temperature history:

80 °C (3 h), 100 °C (3 h), 150 °C (5 h), and a heating rate of 2 °C min^{-1}, followed by maintaining the temperature at 180 °C for 3 h to complete the post curing. This SMP had a T_g of approximately 100 °C and was utilized as the matrix of the fiber-reinforced SMP composite material laminate in this study.

The epoxy-based SMP was reinforced with commercial unidirectional carbon fibers (T300-3 K) produced by Japan Toray Company and had the following mechanical properties: tow number of 3000, tensile strength of 3530 MPa, tensile elasticity modulus of 230 GPa, elongation at break of 1.5%, and density of 1.8 g cm^{-3}.

Unidirectional carbon fiber-reinforced epoxy-based SMP composite laminate. Epoxy-based SMP resin was used to prepare unidirectional fiber-reinforced composites via compression molding, a conventional curing method for resin matrix composites. The volume content fraction of the carbon fiber was v_f = 20%. Compression molding proceeded as follows. The SMP resin was prepared following the same procedure as the bulk SMP, the mixture was preserved after reaction under a low-temperature condition, and the fibers were washed with an organic solution and kept in an oven at 80 °C for 2 h to dry the carbon fiber. Afterward, the release agent was smeared on the mold, and a certain amount of the fiber-reinforced materials was placed in the mold by hand. Then, the SMP resin was injected into the mold, which was closed and pumped vacuum for 2 h subsequently. The mold was transferred into a thermal compressor for solidification following the same temperature history of bulk SMP. After complete solidification, the SMPC laminate was removed from the mold then incised according to the required angles (0°, 90°, and 45°) and sizes. The thickness of the specimens was 2 mm for thermomechanical testing and 1 mm for shape recovery evaluation.

Characterization Methods

The constitutive relation for the overall behavior of SMP and SMPC was thermomechanical performance, which involves three key parameters, namely, stress, strain, and temperature. SMP and SMPC have two characteristics: load carrying of structures at low temperatures below T_g and deformation function at high temperatures above T_g. For the load carrying characteristic of SMP and SMPC, the mechanical properties below T_g need to be studied because the elasticity modulus is relatively high, but the deformation capability is relatively low (<2% overall). Moreover, the linear elastic constitutive relation is mainly considered to be within the range. Therefore, the static mechanical properties of SMP and SMPC are commonly evaluated through conventional characterization methods, such as tensile testing at various temperatures. To evaluate shape memory deformation functions, the following performance indicators of SMPC are required: dynamic mechanical properties and shape memory effect during bending deformation.

Static Mechanical Properties

To characterize the fundamental mechanical properties of the epoxy-based SMP, a tensile test was conducted according to the criterion ASTM-D638. The measuring range of the sensor in the Zwick/Roell tensile machine was 10 kN. The strain of gauge length was measured using a displacement extensometer, which had a temperature-controlled cabinet. Specimen size was tailored according to ASTM D638 and Type IV standard. Specimens were obtained by a laser patterning method that was program-controlled. The displacement rate of the tensile experiment at room temperature (25 °C) was 1 mm min^{-1}, and the displacement rate at high temperature (80 or 100 °C) was 5 mm min^{-1}. The rate at low temperature (−100 °C) was 0.5 mm min^{-1}, and the temperature was controlled by program-controlled liquid nitrogen. The tensile experiment was conducted after 5 min of heat preservation upon reaching the target temperature. The displacement rates were used due to the different temperatures according to the criteria ASTM D3039-14 and ASTM-D638. The mechanical properties of the unidirectional fiber-reinforced SMPC laminate were tested to characterize the fundamental mechanical properties of the SMPC. At room temperature, at least five specimens for each group were used for the experiment. A smart all-digital static resistance strain indicator was utilized to measure the strain, and the Zwick/Roell tensile machine was used to control and record the tensile loading.

Dynamic Mechanical Properties

DMA (DMA2980 TA Instrument) was used to characterize thermodynamic properties, such as glass transition, storage modulus, and T_g, at different temperatures (−50 to 200 °C). T_g is usually defined by using the maximum value of loss angle. The dynamic mechanical properties of the epoxy-based SMP and SMPC were measured, and the three-point bending mode was employed to characterize their fundamental thermodynamic properties. The size, effective span, rate of heating, and frequency of the specimen were $50 \times 9 \times 2$ mm^3, 40 mm, 2 °C min^{-1}, and 1 Hz, respectively.

Scanning Electron Microscopy Observation

Scanning electron microscope (SEM) (Vega3 Tescan) was used to characterize the morphology of the SMPCs at micrometer and nanometer scales and study their features, such as the microstructure of the SMPC. The amplification was from 100 to 10 000 times.

Characterization of the Shape Memory Effect

Given that the shape recovery properties of SMPs can directly determine the deformation properties of their structures, performing a recovery property test is imperative. The shape memory properties of the carbon fiber-reinforced SMPCs were measured through recovery property testing. Specimens with dimensions of $50 \times 15 \times 1$ mm^3 were bent to 180° around a cylinder mold with a curvature radius of 10 mm at T_g (100 °C) in an oil bath. Then, the specimens were kept with external constraint and immersed in water at 25 °C. The deformed shape eventually formed. When immersed back in the oil bath (100 °C), the specimens gradually recovered their original shape and finally stopped at a certain angle θ. The recovery ratio was calculated as (180 - θ)/180.

Characterization in a Ground-Simulated Environment

The mechanical properties after undergoing high/low temperature cycles were conducted with the following experimental conditions: six cycles of high/low temperature under pressure of
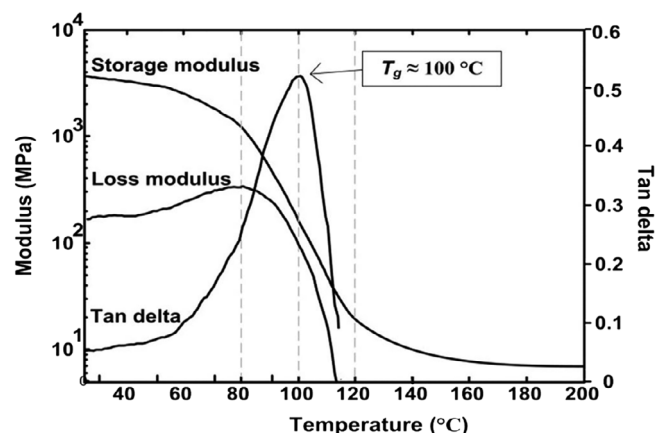
Figure 1. Dynamic mechanical properties of epoxy-based SMP.

1 atm; the temperature limit +80 °C and −100 °C; the effective temperature changing rate around 20 °C min^{-1}. Moreover, the fundamental properties of the SMPC were studied under a special ground-simulated space irradiation environment by Co 60/γ-ray and at an irradiation rate of 300 Gy h^{-1}. The irradiation doses were 1×10^5 Gy (5.5 h) and 1×10^6 Gy (55 h). The irradiation dose of 1×10^6 Gy satisfied the requirement that the material can operate normally in a low Earth orbit for 2 years according to a related space flight industry standard. The irradiation temperature was room temperature (25 °C), and the annealing progress lasted for 24 h.

RESULTS AND DISCUSSION

Thermomechanical Performance of the Pure Epoxy-Based SMP

Dynamic mechanical properties. The dynamic mechanical properties of the epoxy-based SMP were characterized by three-point bending mode at a scanning temperature range of 25–200 °C.

The maximum standard loss angle was used to define T_g. As shown in Figure 1, the T_g of the epoxy-based SMP was approximately 100 °C. At a low temperature (25–80 °C), the SMP was in a glass state, and the modulus was relatively high and stable. The storage modulus at room temperature (25 °C) was 3.51 GPa. When the temperature was from 120 to 200 °C, the SMP was in a viscous rubbery state. During the glass transition process from the glass state to the rubbery state, the storage modulus decreased rapidly from the level of approximately 3 GPa to the magnitude of 10 MPa and finally stabilized at this level in the viscous state. When the SMP was at approximately 80 °C (i.e., $T_g - 20$ °C), it began to exhibit softening on a macroscopic scale. In other words, when epoxy-based SMP is applied to active deformation structures, the structural stiffness and corresponding load carrying capability begin to decrease from this critical temperature point. Furthermore, the deformation capability of the material under T_g influences the recovery capability of active deformation structures. For further details, the static mechanical properties of SMP under T_g are discussed in the following section.

Mechanical properties at varied temperatures. The stress–strain relation of the epoxy-based SMP with $T_g = 100$ °C was investigated, as shown in Figure 2, at temperatures of −100, 25, and 80 °C. The temperature of 80 °C ($T_g - 20$ °C) was selected because the mechanical properties are important at the starting point of T_g according to the dynamic mechanical analysis shown in Figure 1. The SMP exhibited the following mechanical properties: at room temperature (25 °C), the elasticity modulus (extension) was 2.85 GPa, elongation at break was 2.1%, and strength was 60 MPa; at a low temperature of −100 °C, the respective values were 3.0 GPa, 1.55%, and 42 MPa; at a high temperature (80 °C), the respective values were 1.05 GPa, 25.0%, and 19 MPa. The elasticity modulus, elongation at break, and strength of ordinary epoxy-based SMP generally ranged from 1 to 5 GPa, 1 to 3%, and 15 to 65 MPa, respectively. Therefore, the mechanical properties of the epoxy-based SMP at room temperature are
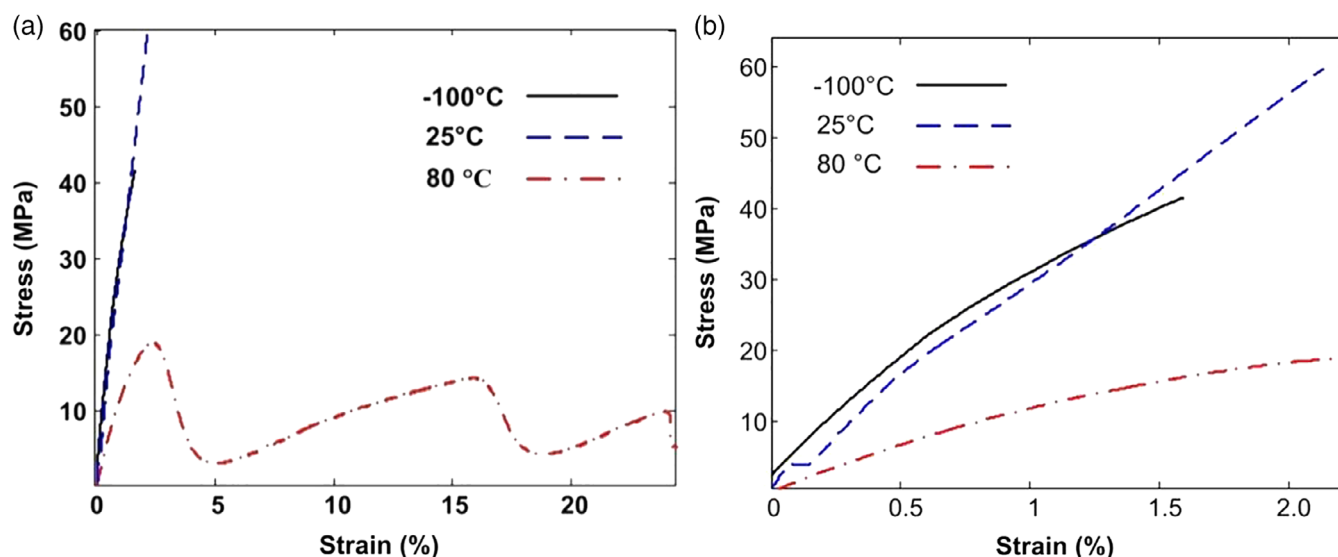

Figure 2. Tensile stress–strain relationship of the epoxy-based SMP at different temperatures (−100, 25, and 80 °C): (a) strain 25% and (b) magnified view of (a). [Color figure can be viewed at wileyonlinelibrary.com]
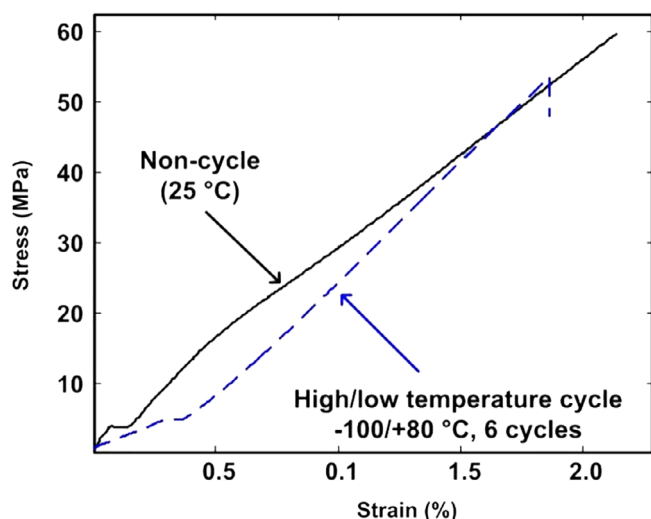
Figure 3. The tensile stress–strain relationship of epoxy-based SMP at 25 °C after high-low temperature cycles (−100/+80 °C, six cycles). [Color figure can be viewed at wileyonlinelibrary.com]

Figure 4. The tensile stress–strain relationship of epoxy-based SMP after radiation, radiation source Co^{60}, γ radial, rate 5 Gy s^{-1}, dose 10^5 Gy (5.5 h) and 10^6 Gy (55 h). [Color figure can be viewed at wileyonlinelibrary.com]

equal to those of conventional epoxy-based polymer materials. Notably, the elongation at break was 2.1% at 25 °C, and this relatively good ductility is helpful for large deformation features. In a low-temperature environment, the elasticity modulus decreased, and the strength and elongation at break dropped dramatically. This trend is similar to that exhibited by conventional resin materials at low temperatures. Although the SMP showed brittleness at an extremely low temperature (−100 °C), the elongation at break (1.55%) was equivalent to the maximal elongation of the conventional resin composite matrix and satisfied the application requirements of composites. In a high-temperature environment (80 °C, $T_g - 20$ °C), the maximal extensional deformation rate reached 25%, and up–down alternating progress was exhibited because the temperature did not approach T_g. As a consequence, the SMP did not become rubbery completely, indicating a nonlinear deformation state combined with plastic deformation and rubbery state.

Mechanical properties undergone high/low temperature cycles. After undergoing six cycles of high/low temperature, the tensile test was conducted with 2 mm min^{-1} at 25 °C. As shown in Figure 3, after the high/low temperature cycles, the elongation at break of epoxy-based SMP decreases slightly from 2.2 to 1.80%. The elasticity modulus is about 3.4 GPa, remaining at the level before the high/low temperature cycles. The strength reduces from around 60 to 54 MPa. In general, the mechanical properties remain relatively stable after experiencing high/low temperature cycles.

Mechanical properties undergone irradiation. As shown in Figure 4, after experiencing irradiation doses of 10^5 Gy and 10^6 Gy, the elongation at break decreases from 2.10% (no irradiation) to 1.50 and 1.15%, respectively. The strength decreased from 60 MPa (no irradiation) to 58 and 44 MPa, and the corresponding elasticity modulus increased from 2.85 MPa (no irradiation) to 4.60 and 3.80 MPa, respectively. It implies that
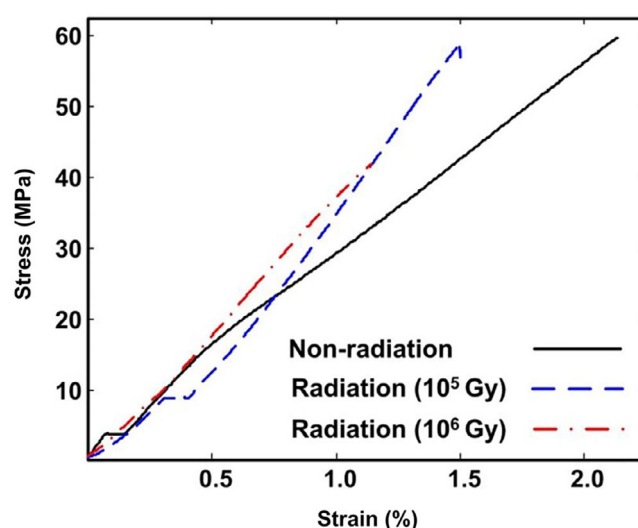
the brittleness is obvious after irradiation. However, the elongation at break (1.1–1.5%) and the strength (40–60 MPa) still meet the requirements for using as structural materials in space.

Mechanical properties at T_g. The deformation performance of the SMP was also evaluated at T_g (100 °C). The stretching rate was set to 5 mm min^{-1}. Figure 5 shows that the maximum deformation of the epoxy-based SMP at T_g reached 55%. The deformation curve presented approximate linearity characteristics, especially for the deformation range of 0–40%. The deformation recovered almost completely (>98%) after unloading the constraints at T_g. Notably, the reversible strain was 55% for the neat epoxy-based SMP. In addition, the elasticity modulus was about 14 MPa.

Mass loss ratio in a vacuum environment. To further investigate the performance to resist vacuum environment in space, the mass loss ratios of epoxy-based SMP as well as their composites were tested in ground stimulation vacuum environment with a pressure intensity of 8.7×10^{-4} Pa for 15 h. The results of the mass loss ratio were 0.15% for SMP without radiation and 0.34% for SMP after radiation. They were 0.36% for SMPC without radiation and 0.65% for SMPC after radiation. Before and after radiation, they were all less than 0.7%, which illustrated that the capacity of resisting the vacuum environment for SMP and SMPC can basically satisfy the requirements in space. Specifically, the mass loss ratio after radiation was higher than the one untreated, which illustrated that radiation can cause damage to the SMP. The mass loss ratio of SMPC was higher than the one of pure SMP, which was caused by bringing into microscopic damage during the preparation process of the SMPC.

Considering the general mechanical properties at the ground simulation environment, the results can be summarized as follows: (1) the toughness remained stable at extremely low temperature of −100 °C; (2) After experiencing high/low alternating
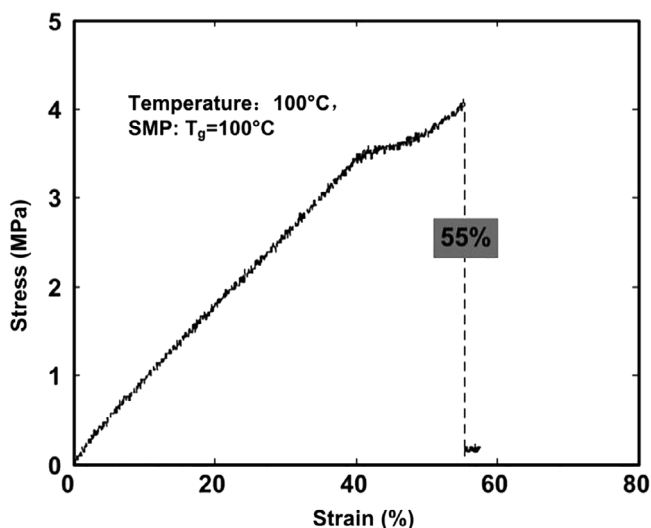
Figure 5. Tensile stress–strain relationship of the epoxy-based SMP at T_g ($T = T_g = 100\ °C$).

temperature cycles, the mechanical properties were still relatively stable; (3) The ability to resist the space irradiation (10^6 Gy, equivalent to 2 years' irradiation doses at low earth orbit) was comparatively stable. These mechanical properties reveal that this epoxy-based SMP could satisfy the basic requirements using as structural materials in space. (4) The SMP and SMPC can satisfy the requirements of vacuum environment in space.

Thermomechanical Performance of the Fiber-Reinforced SMPC

Dynamic mechanical property. The dynamic mechanical properties of the unidirectional carbon fiber-reinforced SMPC were tested by employing the three-point bending mode at a scan temperature range of 25–200 °C. T_g was defined using the standard value of loss angle peak. As shown in Figure 6, the T_g of the carbon fiber-reinforced SMPC was approximately 100 °C, which is equal to that of pure SMP. The thermomechanical performance of the SMPC can be approximately classified into the following
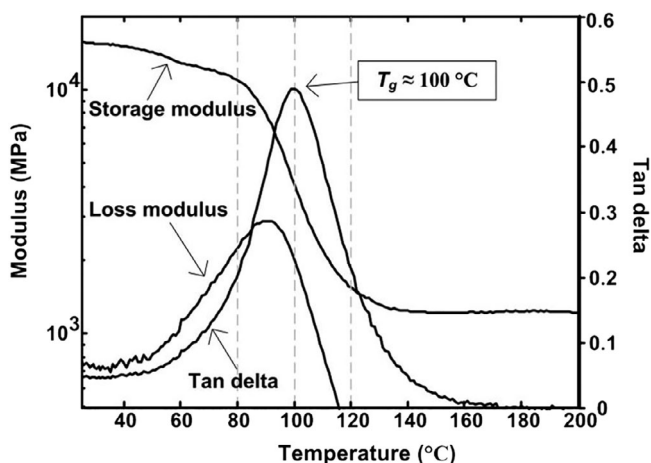

Figure 6. Dynamic mechanical property of the fiber-reinforced SMP composite.

three stages depending on temperature. (1) Within the low temperature range of 25–80 °C, the SMPC was in a glass state with high modulus (>10 GPa) and in a highly stable state. In this glass state, the storage modulus of the SMPC was 15.8 GPa at room temperature of 25 °C. (2) Within the temperature range of 80–120 °C, the SMP matrix of the SMPC was in a rubbery state. Thus, the modulus in the region decreased sharply. In this glassy transition, the storage modulus declined rapidly from the level of 10 GPa to approximately 1 GPa. (3) Within the temperature range of 120–200 °C, the SMP matrix of the SMPC was in a viscous flow state. The modulus was relatively low and maintained at 1 GPa. In all three stages, the modulus of the carbon fiber-reinforced SMPC was higher than that of pure epoxy-based SMP. Therefore, the mechanical properties and shape recovery forces were better than those of bulk SMP, which is the main reason for using fiber reinforcement when SMP is considered for use in deployable structures in space. During glass transition, SMP and SMPC showed the same trend and T_g because the relative evolution of mechanical properties (i.e., tan delta of the DMA curve) is dependent on the SMP matrix but not on the fiber reinforcement.

Tensile mechanical properties. When thermosetting epoxy-based SMPC is to be used for the design of space deployable structures, the basic performance and corresponding parameters as composite lamina or laminate are required, and these include elasticity modulus E_1 and E_2, Poisson's ratio ν_{12} and ν_{23}, and shearing modulus G_{12} and G_{23}.

E_1 and ν_{12}. Samples with fibers having an angle ply of 0° were used to measure the longitudinal parameters of the carbon fiber-reinforced SMPC laminate at room temperature. Elasticity modulus E_1 and Poisson's ratio ν_{12} were obtained by using strain gauges attached on the samples in longitudinal and height directions. As shown in Table I, E_1 is (36.21 ± 2.69 GPa). According to the equal strain assumption, the expression of prediction elasticity modulus is $E_{1-prediction} = E_f v_f + E_m v_m$, where $E_f = 230$ and $E_m = 2.85$ GPa denote the elasticity modulus of the fiber and matrix, respectively, and $v_f = 20\%$ and $v_m = 80\%$ are the volume fraction of the fiber and matrix, respectively. Prediction elasticity modulus $E_{1-prediction}$ is calculated as 48.25 GPa. The experimental result of 36.21 ± 2.69 GPa is lower than that predicted by equal strain assumption models because of the low volume fraction of carbon fibers.

Table I. Mechanical Properties of the SMP Composite in the Longitudinal Direction

Sample	E_1 (GPa)	ν_{12}
Sample 1	40.61	0.55
Sample 2	35.12	0.42
Sample 3	36.89	0.49
Sample 4	33.96	0.39
Sample 5	34.49	0.38
Average value	36.21 ± 2.69	0.45 ± 0.07

Table II. Mechanical Properties of the SMPC in the Transverse Direction

Sample	E_2 (GPa)	v_{23}	G_{23} (GPa)
Sample 1	2.97	0.60	0.93
Sample 2	3.03	0.42	1.07
Sample 3	2.46	0.47	0.84
Sample 4	2.74	0.39	0.99
Sample 5	2.97	0.34	1.11
Average value	2.83 ± 0.24	0.40 ± 0.10	0.97 ± 0.11

Table III. Shear Modulus G_{12} of the SMPC

Sample	G_{12} (GPa)
Sample 1	1.33
Sample 2	1.22
Sample 3	1.25
Sample 4	1.40
Sample 5	1.34
Average value	1.31 ± 0.07

E_2, v_{23}, and G_{23}. Samples with a fiber angle ply of 90° were used to evaluate the transverse parameters of the carbon fiber-reinforced SMP composites at room temperature. Transverse elasticity modulus E_2 and Poisson's ratio ν_{23} were obtained by using strain gauges attached in the transverse direction (perpendicular to the fiber direction) and in the thickness direction. The SMPC on this plane was regarded as a transversely isotropic material because the circular sections of carbon fibers distribute randomly on the plane perpendicular to the fiber direction. The formula $G_{23} = E_2/[2(1 + v_{23})]$ was used to obtain G_{23} indirectly through the experimentally tested elasticity modulus E_2 and Poisson's ratio ν_{23}, as shown in Table II. Transverse elasticity modulus E_2 and the modulus of pure epoxy-based SMP (2.85 GPa, Figure 2) were approximately equal. Shear modulus G_{23} calculated from E_2 and ν_{23} was approximately 1 GPa, which is also approximately equal to the shear modulus of the pure epoxy-based SMP at room temperature. The two results imply that the SMP matrix undertakes the main deformation of the material because the elasticity modulus of the SMP matrix is much lower than that of carbon fibers. Therefore, the deformation of the carbon fibers can be neglected.

G_{12}. To obtain shearing modulus G_{12}, samples with a fiber angle ply of 45° were selected to test the relationship between shearing stress and shearing strain. Longitudinal strain ε_x and strain ε_y in the vertical direction were tested by strain gauges attached to the test lead in longitudinal and vertical directions, respectively. The corresponding loading values, P, were recorded by a force sensor. G_{12} was obtained using the formula $G_{12} = \triangle P/[2bh(\triangle\varepsilon_x - \triangle\varepsilon_y)]$, where b is the width of the samples, h is the thickness of the samples, and $\triangle\varepsilon_x$ and $\triangle\varepsilon_y$ are the loading increments in the longitudinal direction and in the direction perpendicular to the longitudinal direction, respectively. The results of shear modulus value G_{12} of the SMPC are shown in Table III. The value is close to G_{23} and the shear modulus of pure epoxy-based SMP. This result implies that the SMP matrix undertakes the major shear deformation. This condition is the major reason why only the shearing deformation of the SMP matrix was considered whereas that of reinforced fibers was neglected when the system strain energy was calculated in Ref. 45.

Those above mechanical properties (i.e., elasticity modulus E_1 and E_2, Poisson's ratio ν_{12} and ν_{23}, and shearing modulus G_{12}) have completely covered the five independent variables for transverse isotropy composite laminate, which are essential for the design of various composite structures. With those five independent variables, the stiffness matrix E of the unidirectional carbon-fiber-reinforced SMPC laminated plate was obtained. Furthermore, based on the mechanical properties of unidirectional fiber-reinforced SMPC laminated plate, the symmetric and anti-symmetric angle-ply laminated SMPC plate can be designed, which can be used to fabricate complex releasing or deployable structures in space. When this SMPC laminated plate was employed to fabricate the deployable structures (e.g., hinges or trusses), the stiffness in the recovered state can also be predicted by using those five independent variables. In summary, the characterization of the five independent variables for transverse isotropy SMPC laminate may promote development of SMPC structures with huge deformation.

Bending Deformation Behavior of the SMPC Due to Microbuckling

To visually describe the bending deformation behavior of the fiber-reinforced SMPC laminate, its deformed shape was obtained following the procedure of the shape recovery property test in Section 2.2. Figure 7 shows its bending configuration due to the postmicrobuckling of carbon fibers. The buckled fibers exhibited a regular sinusoidal wave shape with obvious wavelengths and amplitudes [see Figure 7(b)], which are the basis to obtain as high as 10% macroscale nominal compression strain for SMPC laminate. Below the critical failure strain of carbon fibers, the microbuckling patterns were reversibly associated with the shape memory deformation cycles on the macroscale. By contrast, beyond the critical failure strain of the carbon fibers, the fibers broke in the areas of maximum amplitudes of buckled sinusoidal-waved fiber bundles.

Microscale buckling is the main mechanism to obtain large macroscale deformation for soft composites.[44,45] As illustrated in Figure 8, the SMPC laminate with a certain thickness t was bent and exhibited flexural deformation on the $x - z$ plane by moment M_{xz} at a certain curvature k. The total deformation process can be classified into three stages (nonbuckling, postmicrobuckling, and failure zones), which are divided by two critical curvatures (critical buckling k_{cb} and critical failure k_{cf}) as follows. First, from the plain state, an SMPC laminate is bent from the zero curvature to critical curvature, and the neutral surface is located on the middle surface of the cross section. Thus, all deformation mechanisms follow the rules of classic composite mechanics. All the fibers are straight [see Figure 8(a)]. Second, beyond the critical curvature indicated in our previous study,[45]
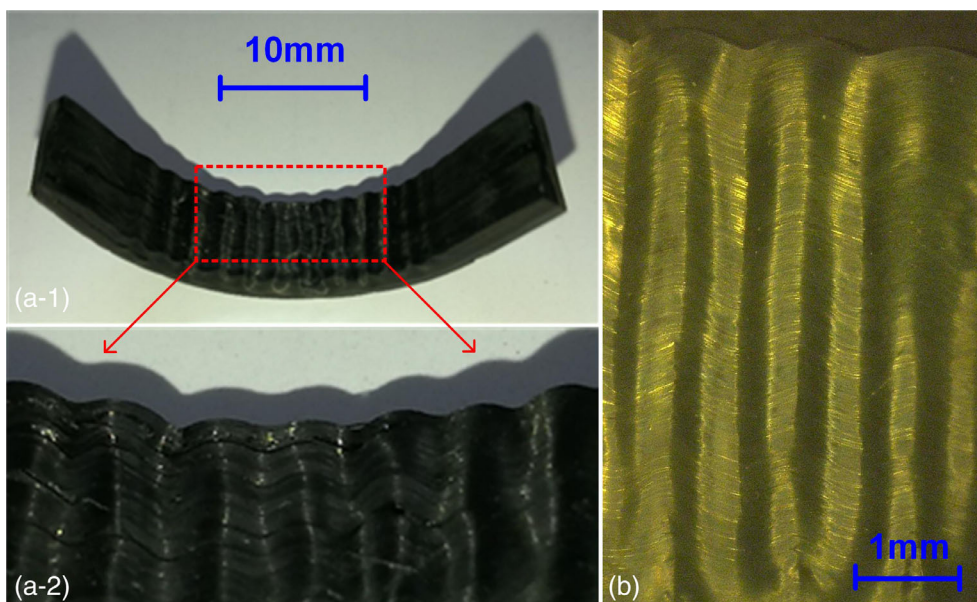
Figure 7. Bending deformation of the unidirectional fiber-reinforced SMPC due to the microbuckling of carbon fibers: (a) photographs of macroscale bending (thickness: 2 mm; bending radius: 20 mm, x–y plane is defined in Figure 6); (b) optical microscopic image of typical microbuckling configuration. [Color figure can be viewed at wileyonlinelibrary.com]

microbuckling occurs, and the critical bending neutral surface moves toward the outer surface, which is in a state of tensile stress. By contrast, in the area around the inner surface, the microbuckling of fiber bundles occurs under the relative high macroscale compressive strain [see Figure 8(b)]. In this way, the SMPC laminate can obtain a maximum macroscale compressive strain of as high as 10% on its inner surface. Third, the SMPC laminate is further bent to and beyond the critical curvature where failures start to occur [see Figure 8(c)], and the typical forms of failure include fiber breaks, SMP matrix cracks, delamination between fibers and the matrix, and gross failure of the SMPC laminate. Failure of SMPC laminates should be avoided in actual engineering applications. Thus, the critical conditions and failure mechanism should be studied to guide SMPC design. The deformation mechanism around the curvature of critical buckling k_{cb} has been studied through analytical and experimental methods.[45] Therefore, the deformation behavior around the curvature of critical failure k_{cf} was preliminary investigated through experimental characteristics in this study.

The SMPC specimens (thickness: 1 mm) were bent to a series of curvatures, namely, 50, 25, 10, 5, and 2.5 mm. The microbuckling of the specimens formed various patterns with different amplitudes and wavelengths. The deformation cycles of the shape memory effect were at least 20 times for all tested specimens. All specimens were bent to a curvature radius of approximately 50 mm to obtain a relatively plain surface to perform optical microscopic observation magnified at 100 times by a microscope, as shown in Figure 9. SMPC failure was defined as the onset of the first fiber breakage. As shown in Figure 9(a–c), after the bending deformation of SMPC specimens at curvature radii of 50, 25, and 10 mm, no failure occurred for all fibers, matrix, or their interfaces. This result suggests that the SMPC specimens work normally even after undergoing more

than 20 flexural deformation cycles. Thus, the corresponding macroscale strains of the SMPC laminate are lower than the failure limits of SMPC materials on the microscale. Figure 9(c-1) shows the height distribution testing results of microbuckling from the side view for the SMPC specimens. The peak–peak amplitudes were approximately 200 μm. Considering the further evolutions of microbuckling under large macroscale strain, Figure 9(d) shows nonfailure coexisting with failure distributions of SMPC microbuckling at a curvature radius of 5 mm, wherein the corresponding strain could be considered the critical strain of microbuckling failure. In a more serious situation, as shown in Figure 9(e), namely, at a curvature radius of 2.5 mm, almost all of the fibers broke at an even higher macroscale strain, which could be regarded as the failure strain. The strains of critical failure and failure are discussed in detail in Figures 10 and 11.

Figure 10 shows the shape recovery sequence of an SMPC specimen with an initial curvature radius of 5 mm in a hot water bath (100 °C) after undergoing more than 20 deformation cycles. The curved SMPC specimen was immersed in hot water and began to deploy in approximately 2–3 s. Figure 10(a) indicates the microbuckling patterns of the zoomed-in bending area where the sinusoidal wave shapes were obvious. Figure 1(b–e) shows the preliminary shape recovery stages with high deformation velocity. With the gradual deployment of SMPC specimens, the amplitudes of the sinusoidal wave shapes for microbuckling decreased slowly. At the final steady state, as shown in Figure 10(f), the SMPC specimens recovered to a straight and plain state, and all the areas with microbuckling vanished, except for the central areas. Figure 10 (f–1) shows the magnified optical microscopic image for the central areas within the dashed rectangle of Figure 10(f). In several nonfailure areas, the fibers, matrix, and conjunction of
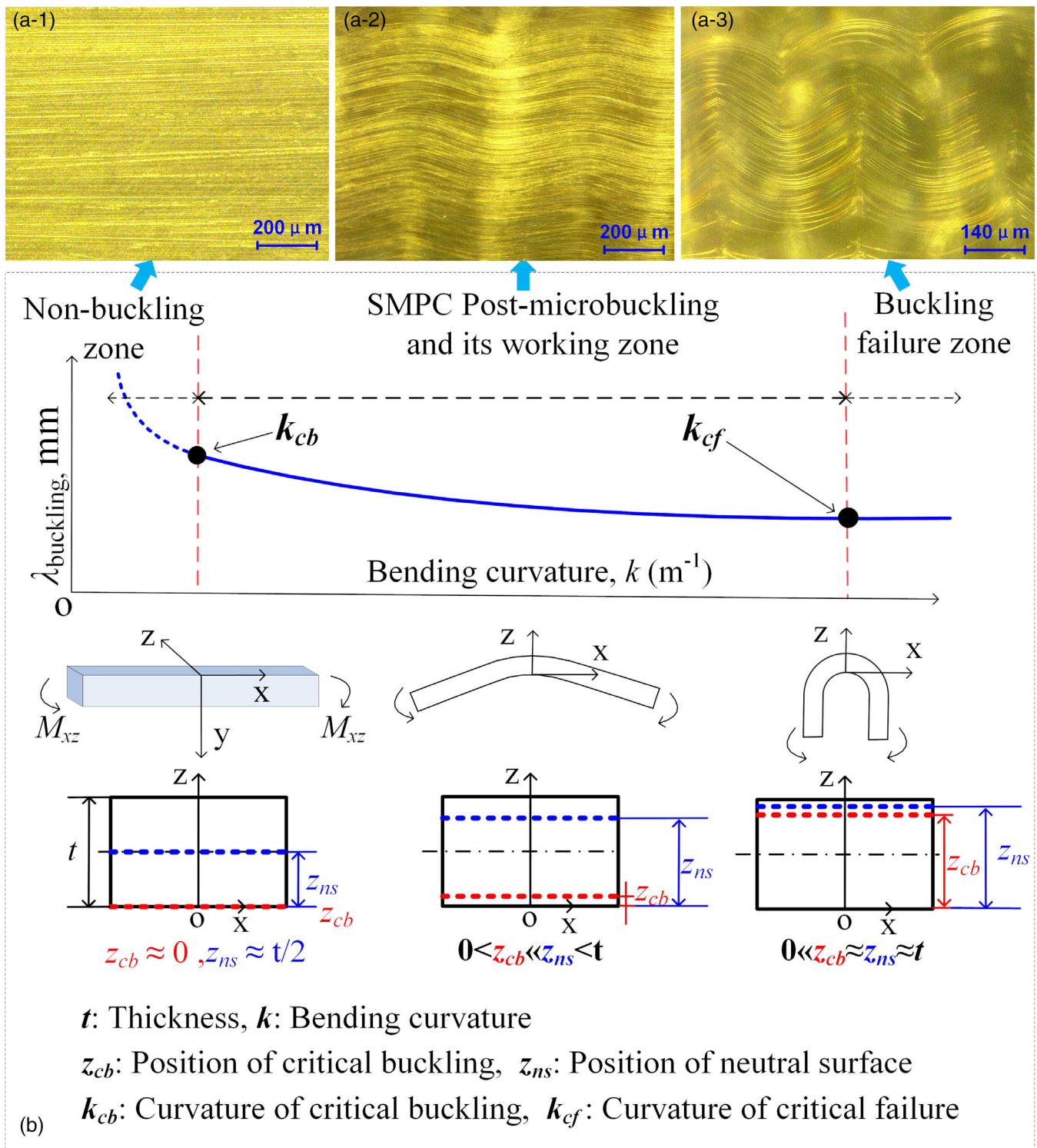
Figure 8. Illustrations of the mechanisms of the flexural deformation of the SMPC laminate; optical microscopic image of typical microbuckling configuration: nonbuckling (a-1), postbuckling (a-2), and failure (a-3); (b) Schematic illustration of the analytical model [Figure 8(b) is modified from Ref. 46]. [Color figure can be viewed at wileyonlinelibrary.com]

fibers and matrix were in perfect working order [see the magnified image in Figure 10(f-1-1)] after experiencing more than 20 deformation cycles at a bending curvature radius of 5 mm with a specimen thickness of 1 mm. Meanwhile, several typical

failure characteristics of composites were observed, including fiber break, delamination between fibers and matrix, and SMP matrix cracking, as shown in the magnified image in Figure 10 (f-1-2).
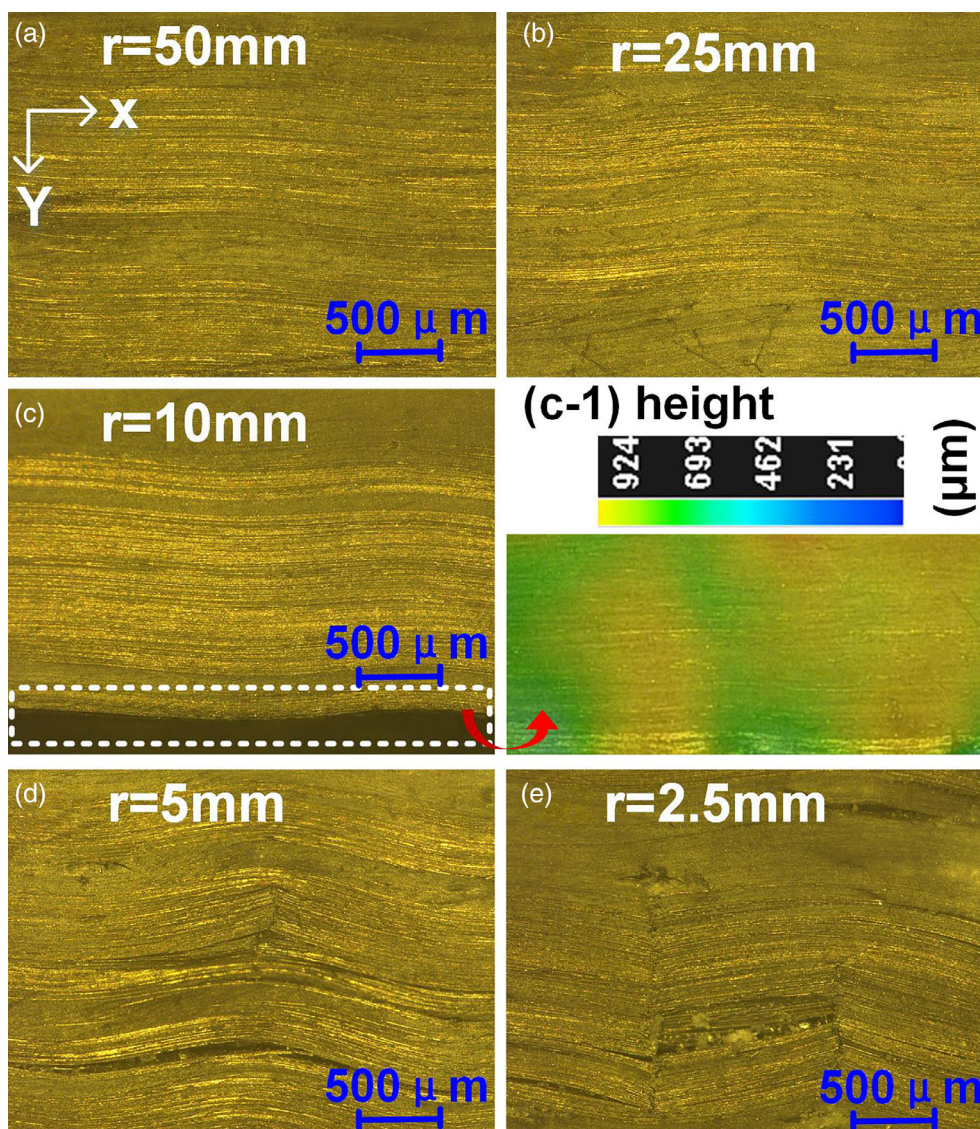
Figure 9. Optical microscopic images of microbuckling patterns of SMPC after undergoing 20 bending deformation cycles at a series of curvature radii: 50, 25, 10, 5, and 2.5 mm (specimen thickness: 1 mm, the x–y plane is defined in Figure 6). [Color figure can be viewed at wileyonlinelibrary.com]

Furthermore, to further evaluate the evolutions of characteristics for SMPC failures at an even smaller curvature, another specimen (thickness of 1 mm) with a curvature radius of 2.5 mm was employed and operated for more than 20 deformation cycles. Figure 11 indicates the recovered shapes of this SMPC specimen with an initial curvature radius of 2.5 mm. The fibers in the bending deformation areas were bent and twisted into the shape of a skew curve. Most of the distorted carbon fiber bundles broke beyond 20 deformation cycles. The bottom row of Figure 11 lists the stepwise magnified SEM images of the distorted fibers in the central areas of bending deformations of Figure 11(a). In Figure 11(b), the collapsing distributions of carbon fiber bundles are obvious, implying that the distortions were serious and the locally distributed strains were high. As shown in Figure 11(c,d), at the peak locations of sine waves, the carbon fiber bundles broke in a timely manner that reflected the brittle break caused by the high local strains in such locations.

According to eq. (43) in our previous study,[45] the maximum strain of SMPC in the postmicrobuckling state at the inner compressing side ($z = 0$) can be derived as $\varepsilon_{\max} = M\left(\sqrt{1 + 2kt/M} - 1\right) - kt$, where $M = v_m G_m/(v_m E_m + v_f E_f)$, thickness t, bending curvature k, elasticity modulus of matrix E_m, shear modulus of matrix G_m, volume fraction of matrix v_m, elasticity modulus of fibers E_f, and volume fraction of fibers v_f. According to the mechanical test results in the aforementioned section, elasticity modulus $E_m = 14$ MPa, and shearing modulus $G_m = 5$ MPa. The volume fraction of matrix $v_m = 20\%$, and the elasticity modulus of fibers $E_f = 230$ GPa. Accordingly, considering the condition of reversible deformation of SMPC, namely, curvature $k = 100$ m^{-1} (curvature radius $R = 10$ mm) and $t = 1$ mm, the calculated maximum strain $\varepsilon_{\max}$ is 9.6%. Alternately, considering the condition of critical failure of SMPC, namely, curvature $k = 200$ m^{-1} (curvature radius $R = 5$ mm)
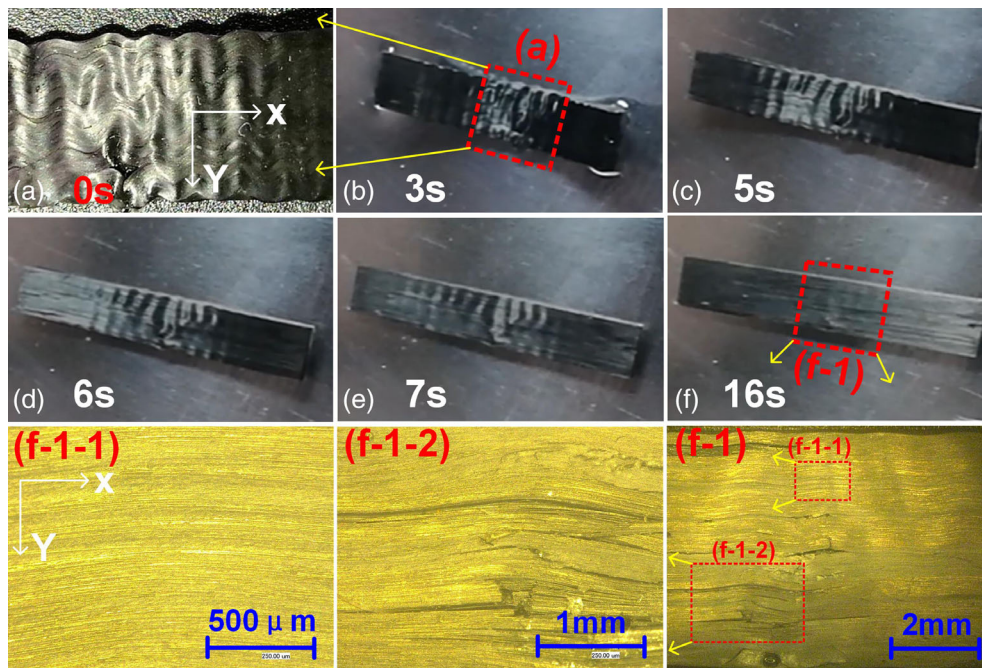
Figure 10. Snapshots of the shape recovery sequence of an SMPC specimen with an initial curvature radius of 5 mm in hot water (100 °C) after undergoing more than 20 deformation cycles (specimen thickness: 1 mm, the x–y plane is defined in Figure 6). [Color figure can be viewed at wileyonlinelibrary.com]
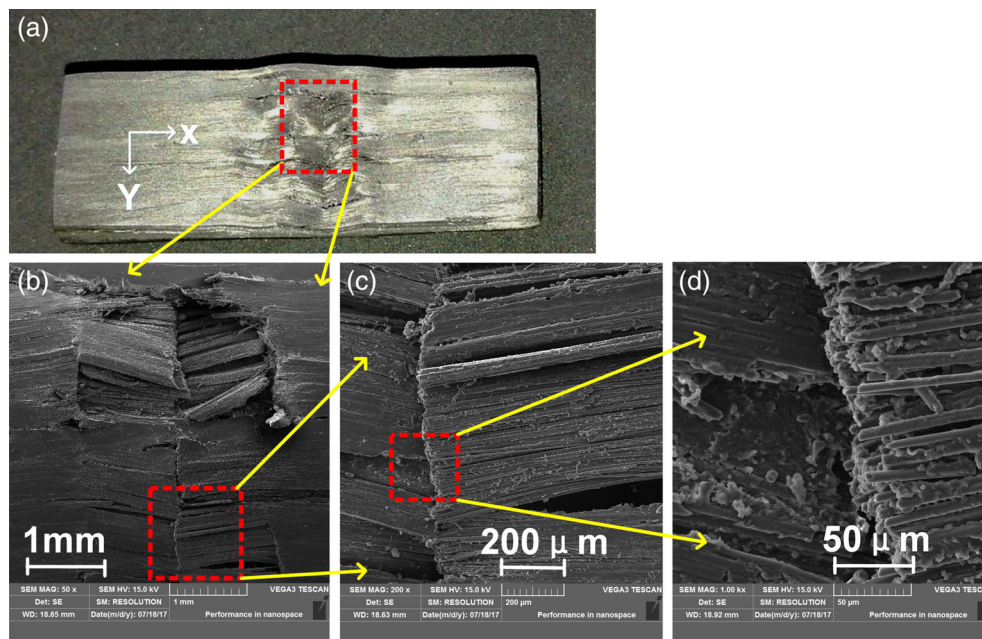

Figure 11. Recovered shapes of an SMPC specimen with an initial curvature radius of 2.5 mm after undergoing more than 20 deformation cycles (specimen thickness: 1 mm, the x–y plane is defined in Figure 6). [Color figure can be viewed at wileyonlinelibrary.com]

and $t = 1$ mm, the expression of maximum strain ε_{max} cannot be obtained because the storage strain energy of failed fibers or the SMP matrix cannot be given according to Ref. 45.

In summary, for SMPC laminates with a thickness of 1 mm undergoing more than 20 deformation cycles, no failures for the curvature radii of 50 mm [Figure 9(a)], 25 mm [Figure 9(b)], and 10 mm [Figure 9(c)] were observed. Thus, the specimen with a

thickness of 1 mm and bending radius of 10 mm (the maximum strain was approximately 9.6%) could be selected for the design of deployable structures, which were also used to evaluate the shape memory effect experiencing numerous deformation cycles in the next section. For the specimen with a thickness of 1 mm and a curvature radius of 5 mm, nonfailure coexisted with failure distributions (Figures 9(d) and 10). Thus, this condition could be

considered as the critical state of microbuckling failure. At a small curvature radius of 2.5 mm, comprehensive distributions of serious failures in the central bending areas were observed [Figures 9(e) and 11], and the strain distributions were difficult to describe.

Note that, to obtain large-deformation ability, the volume faction of reinforced fibers v_f of SMPC is usually 20–40%, but it is usually 60% for ordinary carbon-fiber-reinforced polymer composite. Actually, the material constant $M = v_m G_m/(v_m E_m + v_f E_f)$, which covers the influence of volume faction of reinforced fibers, is used to evaluate the influence in the deformation behavior. When v_f increases, the critical buckling curvature k_{cb} and critical buckling strain ε_{cb} will reduce. It indicates that the formation of microbuckling will be easier because of the decrease of the support of the SMP matrix. Accordingly, the maximum macroscale compressive strain at the inner surface will be larger when v_f increases.

Shape Memory Properties of the SMPC Undergoing Bending Deformation

To apply fiber-reinforced SMPC for active deformation structures in space, an investigation of the shape recovery performance undergoing radiation is necessary. To evaluate the shape recovery of the SMPC upon heating, an SMPC specimen with dimensions of $50 \times 15 \times 1$ mm^3 was predeformed with a curvature radius of 10 mm (as described in the aforementioned section) at 100 °C in an oil bath, cooled at 25 °C with an external constraint, and finally immersed back in the oil bath to record the deformation process. Figure 12 reveals the relationship of the recovery ratio and time at various shape recovery cycles (1st, 5th, 10th, and 25th cycles) for the SMPC without undergoing radiation at T_g temperature of 100 °C. Figure 13 shows the same performance with the same conditions for the SMPC undergoing radiation (radiation source: Co60, γ radial; rate: 5 Gy s^{-1}; amount: 10^6 Gy; time span: 55 h) to simulate the maximum amount of radiation

Figure 13. Evolutions of the shape recovery performance of the SMPC undergoing radiation at varied shape recovery cycles (radiation source: Co60, γ radial rate: 5 Gy s^{-1}; amount: 10^6 Gy (55 h), $T = T_g = 100$ °C). [Color figure can be viewed at wileyonlinelibrary.com]

dose within 2 years at a low Earth orbit without any radiation protection.

As shown in Figure 12, for a certain single cycle of the SMPC, the curve of recovery angle and time showed a nonlinear relationship. (1) At the initial stage of recovery, the SMPC temperature did not achieve the T_g temperature. Thus, the deformation recovery speed was low. (2) At the middle stage, the SMPC temperature fully achieved the T_g temperature, and the recovery speed increased. (3) At the final stage, the material recovery ratio was higher than approximately 90%. The recovery speed of SMPC decreased rapidly and gradually stabilized to a stationary state. Furthermore, considering the evolutions of the shape recovery performance of the SMPC specimen during numerous recovery processes, the recovery speed basically remained stable within five cycles, and the recovery ratio reached 100%. When the number of recovery cycles was more than five, due to the training effect (i.e., the optimization mechanism of the SMP/fibers' microscopic deformation was gradually affected after several shape recovery cycles), the recovery speed gradually increased within 10 cycles. When the number of recovery cycles was between 10 and 25 times, the relatively high recovery speed remained stable in general, and the recovery ratio was maintained at above 95%. Finally, the shape recovery ratio was not only related to the number of shape recovery cycles but also strongly influenced by the SMPC temperature. When the SMPC temperature was above T_g, the shape recovery ratio and speed were relatively high. The shape recovery ratio was maintained above 97% at above T_g, decreased to approximately 85% at T_g −10 °C, and further dropped to approximately 67% at T_g −15 °C. At the T_g temperature of −30 °C, the shape recovery ratio was only 40% approximately. With decreasing temperature, the corresponding shape recovery speeds decreased.
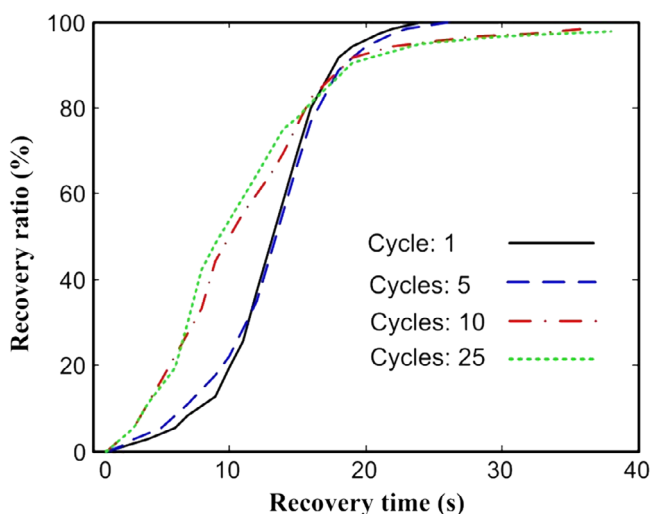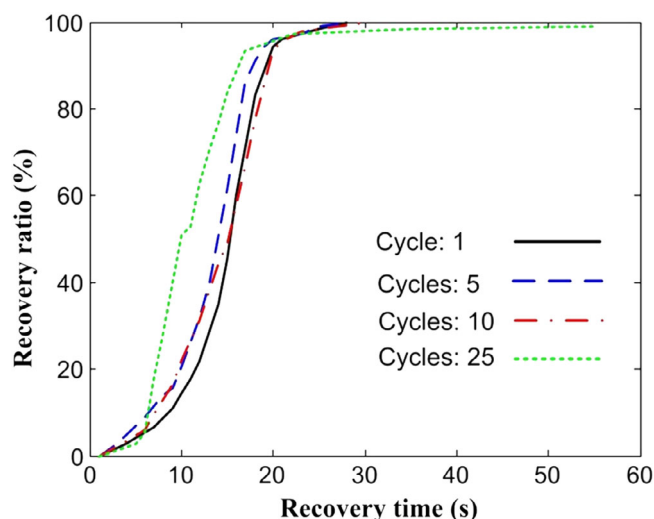

Figure 12. Evolutions of the shape recovery performance of the SMPC specimen without undergoing radiation at varied shape recovery cycles ($T = T_g = 100$ °C). [Color figure can be viewed at wileyonlinelibrary.com]

As shown in Figure 13, the shape recovery properties of another SMPC specimen undergoing 10^6 Gy irradiation were nearly
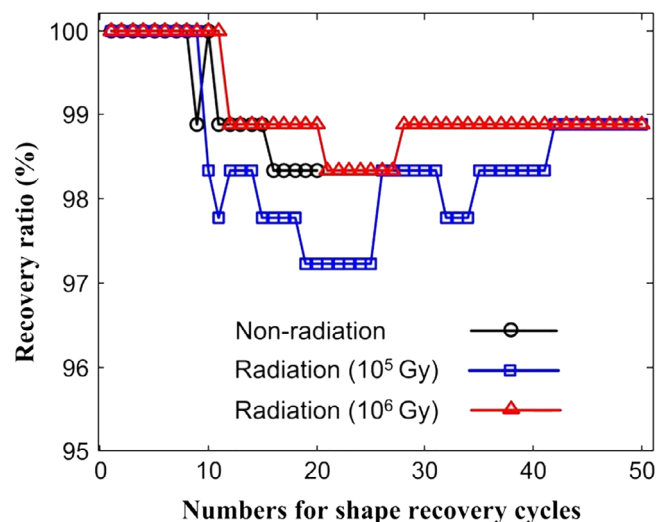
Figure 14. Shape recovery ratio of the SMP composite under different radiation amounts. Radiation source: Co60, γ radial rate: 5 Gy s^{-1}; amount: 10^5 Gy (5.5 h) and 10^6 Gy (55 h, $T = T_g = 100\,°C$). [Color figure can be viewed at wileyonlinelibrary.com]

similar to those of a specimen without radiation (Figure 12). Its deformation process also involved slow deformation, followed by fast linear deformation and slow achievement of the stable state.

A series of the recovery ratios of the SMPC specimens was investigated with different irradiation doses. As shown in Figure 14, the shape recovery ratios were almost 100% in the first 10 shape recovery cycles regardless of whether the SMPC specimens underwent irradiation or not. This condition illustrates that SMPC can completely recover in a small number of cyclic deformation, and the recovery ratio does not decay. Slight residual deformation occurred in the SMPC when the number of shape recovery cycles was more than 10 times and less than 50 times. However, the deformation ratio was maintained at a level higher than 97%. Notably, decay regularity had no relation with irradiation dose.

In summary, microbuckling and the associated bending deformation are reversible after undergoing numerous shape recovery cycles, and this mechanism is proposed to be used for the deployment of SMPC structures in space. Furthermore, compared with the SMPC without radiation, the overall shape memory effects of the SMPC undergoing radiation, such as recovery speed and recovery ratio (>97%), did not decline obviously after undergoing 10^6 Gy of irradiation. This phenomenon proves that SMPC can still maintain shape memory effects even after exposure to the radiation environment within 2 years at low Earth orbit without any radiation protection.

DISCUSSION, FUTURE WORK, AND APPLICATIONS

Due to the microbuckling of fibers in compressive area, the fiber reinforced SMPC can obtain as high as around 10% macroscale nominal compressive strain, which is much higher than traditional fiber-reinforced composite without shape memory effect (maximum strain around 2%). When the values of material parameters (i.e., elastic modulus of the SMP matrix, volume
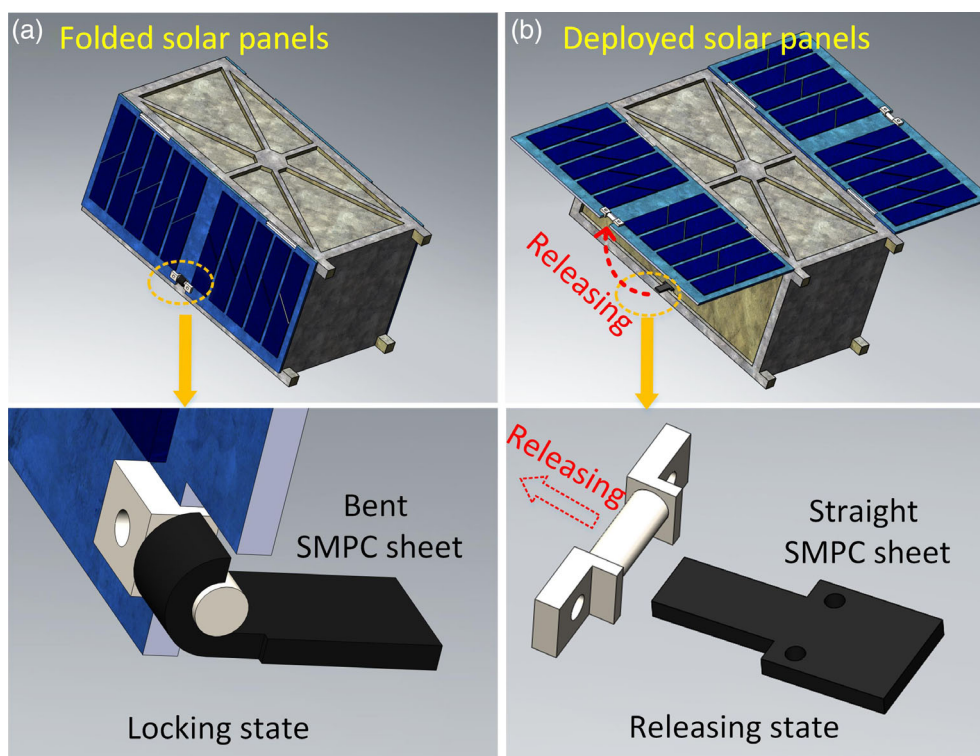

Figure 15. Application of SMPC in the releasing mechanism on a nanosatellite: (a) a small sheet of SMPC bent into a hook shape to lock the small solar panel; (b) the bent hook recovers to the original straight state to release the solar panel. [Color figure can be viewed at wileyonlinelibrary.com]

fraction of fibers) reduce, the formation of fiber microbuckling will be easier, and the deformation will be accordingly larger. During the gradual bending process of SMPC with bending curvature increasing from zero to a certain large value, the fibers at the inner surface of the cross section of SMPC will undergo three stages, namely nonbuckling, postbuckling, and failure, which are accordingly divided by two critical values of curvatures, namely the critical buckling curvature and the critical failure curvature. The critical buckling curvature has been analytically predicted and experimentally validated. The critical failure curvature is a problem regarding strength, which should be tested through systematic experiments.

The bending large-deformation theories of SMPC have been studied in our previous papers.[45,46] In this study, the experimental characterization has provided the thermomechanical properties of pure SMP and unidirectional carbon-fiber-reinforced SMPC, which are the basis for stiffness design of unidirectional fiber-reinforced SMPCs and angle-ply laminated SMPCs in original and recovered shape. Furthermore, the bending deformation behavior was also experimentally characterized to validate the key theoretical predictions of the microbuckling, such as the evolution process from nonbuckling to postmicrobuckling, and final failure. However, due to the complexity of the shape memory effect during a thermomechanical cycle of SMPCs, the following studies still need to be carried out in the near future.

Stiffness Design Approach of SMPCs in the Soft State

The standard approach and flow of stiffness design should be established for fiber-reinforced SMPCs with bending large-deformation, including the following key parameters (1) structural parameters: diameter, volume fraction of reinforced fibers; length, thickness, and width of SMPC plate; bending curvature, and so forth; (2) material properties: elasticity modulus, shearing modulus of matrix as well as reinforced fibers, and so forth; and (3) deformation performance: position of neutral surface, position of critical buckling, half-wavelength, amplitude, shearing strain, macrocompressive strain, macrotensile strain, strain of fibers, total energy, and actuation moment, and so forth.

Strength Criterion of SMPCs in the Soft State

The strength criterion should be established for SMPCs in bending and compression large-deformation states. The safety factors should also be provided. Standard methods of experimental characterization of compressive strength for SMPCs in the soft state should be provided. A series of values of compressive strength should be provided for various SMPCs at different temperatures.

Stiffness Prediction of SMPCs in the Predeformed Hard State

The current study in the stiffness of SMPCs in the predeformed hard state is vacant. In the predeformed hard state for SMPCs in bending and compression large-deformation states, the stiffness prediction should consider that the microbuckling fibers coexist with the straight fibers. Moreover, the bending stiffness may be different when applying the moment M_{xz} in the positive or negative direction as shown in Figure 8. Hence, theoretical prediction and experimental evaluation of the stiffness of SMPCs in the predeformed state should be investigated in the near future.

Creep and Relaxation Characteristic of SMPCs in the Predeformed Hard State

The strain energy is stored in the predeformed hard state of SMPCs, and the creep and relaxation will occur in the long-term package process for the high molecular polymer matrix in SMPCs. When the SMPCs are used for the releasing mechanism, the long-term locking stiffness is sensitive to the viscoelastic characteristic. The creep and relaxation should be considered when designing SMPC locking and releasing devices.

On the basis of the thermomechanical properties and bending large-deformation behavior, the unidirectional fiber-reinforced SMPC laminates could be designed and used for the space deployable structures, such as deployable hinges, trusses, soft solar arrays, and lens hoods. Moreover, they could be used to design and fabricate the releasing mechanism for deployable structures in space. For instance, as shown in Figure 15, a small sheet of SMPC can be bent into a hook shape to lock the small solar panel on a nanosatellite. When the SMPC hook in bent shape is heated, it recovers to the original straight state, and the solar panel is released and then deploys actuated by the torsional springs on the other side. In this application, the predeformed bent shape can be accurately designed, including geometrical parameters (length, width, and thickness), maximum bending radius without SMPC failures, and the associated microbuckling parameters (wavelength and amplitude, etc.). The locking stiffness should also be designed and evaluated for SMPC in the hard state in the predeformed bent shape. Finally, the actuation performance (moments at various temperatures) of SMPC sheet could also be designed and evaluated during the recovering process. In special, another article will be published soon to investigate the design, fabrication, and validation of SMPC used for this locking mechanism on 2 U nano-satellite, where the R&D procedure strictly followed the China aerospace standard.

CONCLUSIONS

In this study, a unidirectional carbon fiber-reinforced epoxy-based SMPC laminate was prepared, and the basic static and dynamic properties were characterized. The morphology, including the postmicrobuckling and failure behavior of the SMPC, was studied, and the corresponding shape recovery properties were measured. The main conclusions are listed as follows:

1. The glass transition temperature of the pure epoxy-based SMP is 100 °C. The elasticity modulus is approximately within the range of 2.5–3.0 GPa, the elongation at break is within the range of 2.0–2.5%, and the strength is approximately 50–65 MPa. The maximum reversible strain at the glass transition temperature reaches 50%, and the corresponding elasticity modulus is approximately 14 MPa.
2. The epoxy-based SMP satisfies the requirements of space environment. For the high/low temperature cycles (−100 to +80°C, six cycles), the mechanical properties remain stable. After enduring Co60 γ-ray irradiation with dose10^6 Gy, the chemical structures and macromechanical properties are stable. The SMP and SMPC can satisfy the requirements of vacuum environment in space.

3. In the dynamic thermodynamic testing, the glass translation temperature is approximately 100 °C, which is similar to that of the pure SMP. The basic mechanical properties of the fiber-reinforced SMP composites at room temperature are $E_1 = 36$ GPa, $E_2 = 2.83$ GPa, $\nu_{12} = 0.45$, $\nu_{23} = 0.40$, $G_{12} = 1.31$ GPa, and $G_{23} = 0.97$ GPa. It is the basis to design the SMPCs with complex structures.

4. The fiber-reinforced SMPC exhibits local microbuckling during bending deformation. The SMPC obtains large reversible macrostrain of as high as approximately 9.6% during bending deformation. Furthermore, the state of critical failure of bending deformation is observed (thickness of 1 mm and bending radius of 5 mm).

5. The recovery speed is basically nonlinear. The recovery ratios approach 100% within the first five deformation cycles and are slightly reduced to 97% within 25 deformation cycles. After undergoing radiation with a dose of 10^6 Gy, several key shape memory properties, such as recovery speed and recovery ratio, are relatively stable.

On the basis of this fundamental research on unidirectional fiber-reinforced SMPC laminate, the SMPC of angle-ply laminated plates, woven laminated plates, or several special laminated structures can be further designed for large deformable structures in space, such as deployable hinges, trusses, soft solar arrays, self-assembly structures in orbit, and releasing mechanism.

ACKNOWLEDGMENTS

REFERENCES

1. Xie, T. *Nature*. **2010**, *464*, 267.
2. Leng, J. S.; Lan, X.; Liu, Y. J.; Du, S. Y. *Prog. Mater. Sci.* **2011**, *56*, 1077.
3. Dubal, D. P.; Chodankar, N. R.; Kim, D. H. *Chem. Soc. Rev.* **2018**, *47*, 2065.
4. Liu, R. Y.; Kuang, X.; Deng, J. A. *Adv. Mater.* **2018**, *30*, 17.
5. Jin, B. J.; Song, H. J.; Jiang, R. Q. *Sci. Adv.* **2018**, *4*, 05195.
6. Lan, X.; Liu, L. W.; Liu, Y. J.; Leng, J. S. *J. Appl. Polym. Sci.* **2018**, *135*, 45978.
7. Wang, X.; Sparkman, J.; Gou, J. H. *Compos. Sci. Technol.* **2017**, *8*, 141.
8. Lian, H. Q.; Chang, W.; Liang, Q. *RSC Adv.* **2017**, *7*, 46221.
9. Lu, H. B.; Yin, J. Y.; Xu, B. *Compos. Part B-Eng.* **2016**, *100*, 146.
10. Huang, C. J.; Peng, J. S.; Cheng, Y. R. *J. Mater. Chem. A.* **2019**, *7*, 2787.
11. Leng, J. S.; Lan, X.; Liu, Y. J.; Du, S. Y.; Huang, W. M.; Liu, N.; Phee, S. J.; Yuan, Q. *Appl. Phys. Lett.* **2008**, *92*, 014104.
12. Leng, J. S.; Huang, W. M.; Lan, X.; Liu, Y. J.; Liu, N.; Du, S. Y. *Appl. Phys. Lett.* **2008**, *92*, 204101.
13. Wei, H. Q.; Zhang, Q. W.; Yao, Y. T.; Liu, L. W.; Liu, Y. J.; Leng, J. S. *ACS Appl. Mater. Interfaces.* **2017**, *9*, 876.
14. Liu, Z.; Cui, A. J.; Li, J. *J. Adv. Mater.* **2019**, *31*, 1802211.
15. Liu, X. Y.; Yuk, H.; Lin, S. T. *Adv. Mater.* **2018**, *30*, 1704821.
16. Zarek, M.; Mansour, N.; Shapira, S.; Cohn, D. *Macromol. Rapid Commun.* **2017**, *38*, 1600628.
17. Ge, Q.; Qi, H. J.; Dunn, M. L. *Appl. Phys. Lett.* **2013**, *103*, 131901.
18. Ge, Q.; Dunn, M. L.; Qi, H. J.; Dunn, M. L. *Smart Mater. Struct.* **2014**, *23*, 094007.
19. Wang, Q. M.; Zhao, X. H. *MRS Bull.* **2016**, *41*, 115.
20. Lagrange, R.; LópezJiménez, F.; Terwagne, D.; Brojan, M.; Reis, P. M. *J. Mech. Phys. Solids.* **2016**, *89*, 77.
21. Bai, J.; Shi, Z. X. *ACS Appl. Mater. Interfaces.* **2017**, *9*, 27213.
22. Feng, X. Q.; Zhang, G. Z.; Zhuo, S. Y.; Jiang, H. Y.; Li, H. J. *Compos. Sci. Technol.* **2016**, *129*, 53.
23. Wang, B. S.; Zhai, W. Z.; Fan, J. B.; Xu, J.; Zhao, W. P.; Feng, X. Q. *Nanoscale.* **2019**, *11*, 6846.
24. Lendlein, A.; Gould, O. C. *Nat. Rev. Mater.* **2019**, *4*, 116.
25. Liu, Y. J.; Du, H. Y.; Liu, L. W.; Leng, J. S. *Smart Mater. Struct.* **2014**, *23*, 023001.
26. Lan, X.; Wang, X. H.; Liu, Y. J.; Leng, J. S. *Smart Mater. Struct.* **2009**, *18*, 024002.
27. Wang, Y. K.; Zhu, G. M.; Xie, J. Q.; Men, Q. L.; Liu, T. T.; Ren, F. *J. Polym. Res.* **2014**, *21*, 515.
28. Rahman, A. A.; Ikeda, T.; Senba, A. *Fibers Polym.* **2017**, *18*, 979.
29. Cuevas, J. M.; Rubio, R.; Laza, J. M.; Vilas, J. L.; Rodriguez, M.; Leon, L. M. *Smart Mater. Struct.* **2012**, *21*, 035004.
30. Guo, J. M.; Wang, Z. Q.; Tong, L. Y.; Lv, H. Q.; Liang, W. Y. *Composites, Part A.* **2015**, *76*, 162.
31. Wei, H. Q.; Liu, L. W.; Zhang, Z. C.; Du, H. Y.; Liu, Y. J.; Leng, J. S. *Compos. Struct.* **2015**, *133*, 642.
32. Fejos, M.; Romhany, G.; Karger-Kocsis, J. *J. Reinf. Plast. Compos.* **2012**, *31*, 1532.
33. Fejos, M.; Karger-Kocsis, J. *Express Polym. Lett.* **2013**, *7*, 528.
34. Ahmada, M.; Singh, D.; Fu, Y. Q.; Miraftab, M.; Luo, J. K. *Polym. Degrad. Stabil.* **2011**, *96*, 1470.
35. Sun, J.; Liu, Y. J.; Leng, J. S. *J. Intell. Mater. Syst. Struct.* **2015**, *26*, 2020.
36. Takeda, T.; Narita, F.; Shindo, Y. *J. Sandwich Struct. Mater.* **2016**, *18*, 113.
37. Takeda, T.; Shindo, Y.; Narita, F. F. *J. Compos. Mater.* **2015**, *49*, 209.
38. Radford, D. W.; Antonio, A. *Strain.* **2011**, *47*, 534.
39. Robinson, P.; Bismarck, A.; Zhang, B.; Maples, H. A. *Compos. Sci. Technol.* **2017**, *145*, 96.
40. Li, F. F.; Liu, L. W.; Lan, X.; Wang, T.; Li, X. Y.; Chen, F. L.; Bian, W. F.; Liu, Y. J.; Leng, J. S. *Int. J. Appl. Mech.* **2016**, *08*, 07.
41. Liu, Y. Q.; Xu, K. G.; Chang, Q. *Adv. Mater.* **2016**, *28*, 7758.
42. Xie, F.; Huan, L. N.; Liu, Y. J.; Leng, J. S. *Polymer.* **2014**, *55*, 5873.

43. Gao, H.; Lan, X.; Liu, L. W.; Xiao, X. L.; Liu, Y. J.; Leng, J. S. *Smart Mater. Struct.* **2017**, *26*, 095001.

44. Leng, J. S.; Wu, X. L.; Liu, Y. J. *Smart Mater. Struct.* **2009**, *18*, 095031.

45. Lan, X.; Liu, L. W.; Liu, Y. J.; Leng, J. S. *Mech. Mater.* **2014**, *72*, 46.

46. Lan, X.; Liu, L. W.; Liu, Y. J.; Leng, J. S. *J. Compos. Mater.* **2019**, https://doi.org/10.1177/0021998319854145.